The Effect of Polymer Matrix on the Catalytic Properties of Supported Palladium Catalysts in the Hydrogenation of Alkynols

Eldar Talgatov [1], Assemgul Auyezkhanova [1,*], Alima Zharmagambetova [1], Lyazzat Tastanova [2], Farida Bukharbayeva [1,3], Aigul Jumekeyeva [1] and Talgat Aubakirov [4]

[1] D.V. Sokolskiy Institute of Fuel, Catalysis, and Electrochemistry, Laboratory of Organic Catalysis, Kunaev str. 142, Almaty 050010, Kazakhstan

[2] Department of Chemistry and Chemical Technology, K. Zhubanov Aktobe Regional University, A. Moldagulova Avenue 34, Aktobe 030000, Kazakhstan

[3] Institute of Natural Sciences and Geography, Abai Kazakh National Pedagogical University, Kasybek bi str. 30, Almaty 050026, Kazakhstan

[4] Higher School of Natural Science, Pavlodar Pedagogical University, Mir Street 60, Pavlodar 140000, Kazakhstan

[*] Correspondence: auyezkhanovaa@gmail.com

Abstract: Palladium catalysts were obtained by the adsorption method involving the sequential deposition of polyvinylpyrrolidone (PVP) and then palladium ions on a modified zinc oxide surface without high-temperature calcination and reduction stages. The immobilized PVP-palladium catalysts were characterized by scanning electron microscopy (SEM), transmission electron microscopy (TEM), Brunauer–Emmett–Teller (BET), infrared spectroscopy (IRS), X-ray powder diffraction (XRD), X-ray photoelectron spectroscopy (XPS), and elemental analysis methods. It was found that the introduction of polymer into the catalyst's composition promotes the dispersion and uniform distribution of active phase nanoparticles (PdO, Pd^0) on the surface of zinc oxide. The catalysts were tested in the hydrogenation of complex acetylene alcohol, 3,7,11-trimethyldodecyn-1-ol-3 (C_{15}-yn) under mild conditions (0.1 MPa, 40 °C). For comparison, studies on stereoselective hydrogenation of the short-chain alcohol 2-hexynol-1 were performed. It was shown that modification of the catalyst with polymer improves its catalytic properties. High C_{15}-alkenol selectivity (98%), activity ($W = 70 \times 10^{-6}$ mol/s), and stability (turnover number (TON) 62,000) were achieved on a Pd-PVP/ZnO catalyst. Varying the active phase made it possible to reduce the metal content without deteriorating the catalytic performance of the catalyst.

Keywords: supported palladium catalysts; polymer-modified catalysts; polyvinylpyrrolidone; catalytic hydrogenation; 3,7,11-trimethyldodecyn-1-ol-3; 2-hexynol-1

1. Introduction

The catalytic hydrogenation of organic compounds is one of the most important processes in the different fields of the chemical industry [1–7]. Based on patent data, within the group of heterogeneous hydrogenation catalysts, palladium is found to be the most prevalent metal component [1]. Among the supported catalysts, the Pd/C and Lindlar catalysts, developed in the last century, are still used in the industry to this day [5–9]. However, the development of well-stable, highly active, and selective nanocatalysts with a low content of noble metals remains a challenge. The immobilization of metal complexes with macromolecular ligands onto inorganic or hybrid supports has attracted considerable attention as a promising approach for the design of heterogeneous catalysts with embedded Pd nanoparticles [10–15]. Such hybrid catalysts have been investigated in the hydrogenation reactions of various unsaturated compounds [16–22]. These catalysts are often prepared in toxic solvents and the palladium is reduced with sodium borohydride.

Nowadays, due to the requirements for eco-friendly chemistry, renewable degradable polymers, such as natural polysaccharides, are used for the synthesis of polymer-protected nanocatalysts [23–25]. Moreover, greener media that limit volatile organic solvents are preferable. Water, being available, is the most relevant environmentally benign solvent.

In our prior works, taking into account the principles of green chemistry, we developed a one-pot method for the synthesis of supported polysaccharides containing palladium catalysts from the water solutions of polymers and metals. The process is carried out under ambient conditions without stages of high-temperature calcination and reduction [16,26–28]. Catalysts can be stored in the air for a long time without losing their original effectiveness. Palladium (Pd^{2+}) in catalysts is reduced by molecular hydrogen directly in the reactor before the introduction of the hydrogenated compound, which greatly simplifies the process. In liquid-phase processes with proper solvent selection, the surface metal–polymer layer of the developed system swells, leading to an increase in the accessibility of all active centers (metal nanoparticles). The hydrogenation process on these types of catalysts in a non-aqueous medium is complicated because the surface polysaccharide-containing layer will be shrunk, which leads to a decrease in the activity of the catalyst.

The advantage of polyvinylpyrrolidone (PVP) is its good solubility in water and organic solvents [15,22] due to the presence of both polar carbonyl groups and the nitrogen atom of the pyrrolidone ring, as well as the nonpolar methylene and methine groups in the ring. It is shown that PVP strongly binds to the metal nanoparticles [29]. These properties can promote the dispersity of metal nanoparticles in supported PVP-modified catalysts at liquid-phase reactions [15,22] and avoid the aggregation and leaching of metals from the support.

The hydrogenation of complex acetylenic alcohols is widely used in fine chemistry to produce biologically active compounds [5,19]. Despite a lot of works that have been published on alkynol hydrogenation, only a small amount have considered the behavior of polymer-stabilized supported catalysts.

The main aim of the present work is to study the effect of the polymer matrix on the properties of low-percentage Pd-PVP/ZnO catalysts in the hydrogenation of complex acetylated alcohols, such as 3,7,11-trimethyldodecyn-1-ol-3 (C_{15}-yn) and 2-hexyn-1-ol, the intermediate products of some biologically active compounds. The process was carried out under optimal conditions (1 atm, 40 °C in ethanol) determined experimentally.
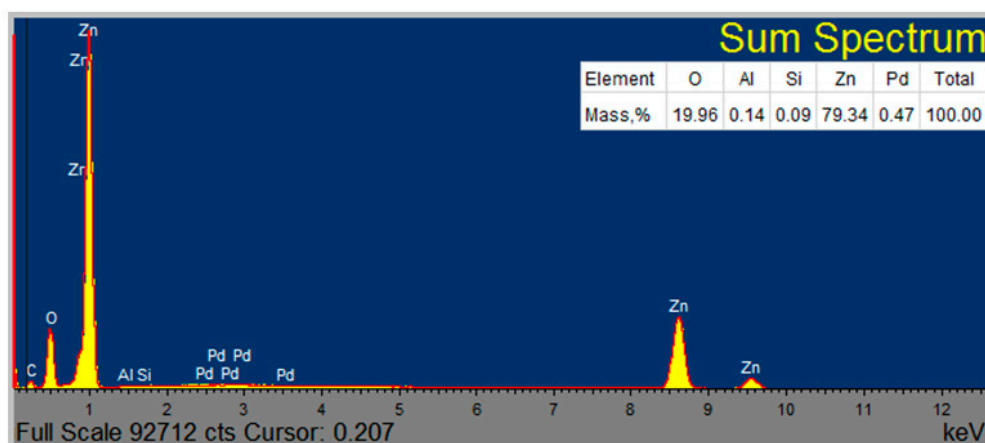
2. Results

2.1. Characterization of Catalysts

The PVP-modified Pd catalysts supported on zinc oxide were prepared by sequential adsorption of the polymer and palladium ions on inorganic oxide. The amount of introduced palladium salt (K_2PdCl_4) and polymer were taken from calculation to obtain Pd-PVP/ZnO catalysts with a Pd content of 0.25–1.00 wt.% and a [Pd:PVP] molar ratio = 1:1. For comparison, similar unmodified Pd/ZnO catalysts were prepared using the same procedure except that the polymer was added. The Pd content in the resulting catalysts was evaluated using the spectrophotometry method. According to the analysis of the supernatant solution collected after the sorption process, approximately 96–99% of the introduced palladium amount was immobilized on the support material. Thus, the palladium content in all catalysts was close to the calculated data and amounted to 0.25–1.0 wt.% of the sum of all components (Table 1).

Table 1. Immobilization of Pd^{2+} ions on PVP-modified zinc oxide precipitated from water solution.

Catalyst	Mass of Palladium in Mother Liquor, mg		The Amount of Pd Absorbed		Pd Content in Catalyst, %
	Before Adsorption	After Adsorption	mg	%	
1%Pd/ZnO	10.1	0.3	9.8	97	1.0
1%Pd-PVP/ZnO	10.1	0.1	10.0	99	1.0
0.5%Pd/ZnO	5.0	0.2	4.8	96	0.5
0.5%Pd-PVP/ZnO	5.0	0.1	4.9	98	0.5
0.25%Pd-PVP/ZnO	2.5	0.1	2.4	96	0.25

The Energy Dispersive X-ray (EDX) elemental analysis results of the 0.5%Pd/ZnO and 0.5%Pd-PVP/ZnO catalysts confirm the data obtained by the spectrophotometry method. The Pd content in the 0.5%Pd/ZnO and 0.5%Pd-PVP/ZnO catalysts were found to be 0.47 and 0.49%, respectively (Table 2). This is close to the value of 0.5 wt.% calculated using the spectrophotometry method. It should be noted that no peaks of chlorine were observed on the EDX spectra of catalysts (Figure 1). This can be explained by the fact that after the adsorption process, the resulting catalysts were washed with distilled water until the filtrates attained a neutral reaction with the chloride ions.


(**a**)
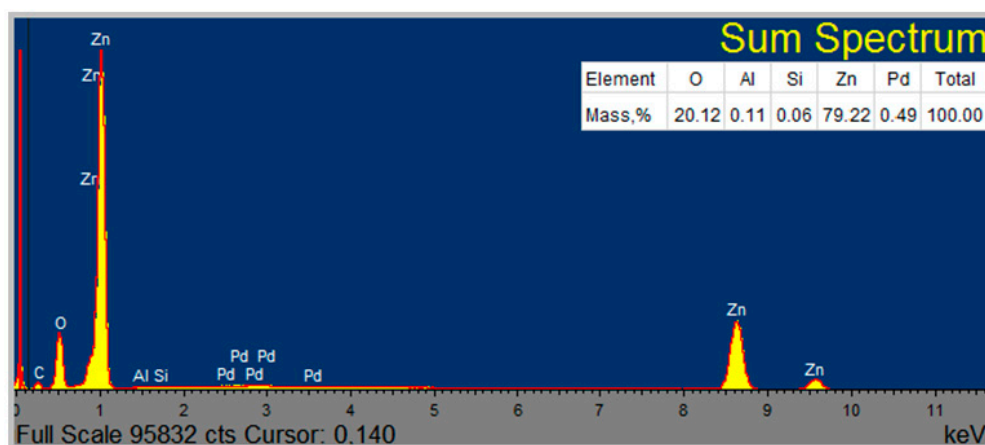
(**b**)

Figure 1. EDX elemental analysis results of the 0.5%Pd/ZnO (**a**) and 0.5%Pd-PVP/ZnO (**b**) catalysts.

Table 2. BET surface area of the ZnO, 0.5%Pd/ZnO, PVP/ZnO, and 0.5%Pd-PVP/ZnO samples.

Sample	Surface Area, $m^2 g^{-1}$
ZnO	9.8
PVP/ZnO	5.2
0.5%Pd/ZnO	9.3
0.5%Pd-PVP/ZnO	5.9

Figure 2 shows the scanning electron microscopy (SEM) and EDX elemental mapping images of Zn and Pd from the 0.5%Pd/ZnO and 0.5%Pd-PVP/ZnO catalysts. Both elements are homogeneously distributed corresponding to the SEM images. This suggests that Pd is homogeneously deposited on both unmodified and PVP-modified zinc oxide.
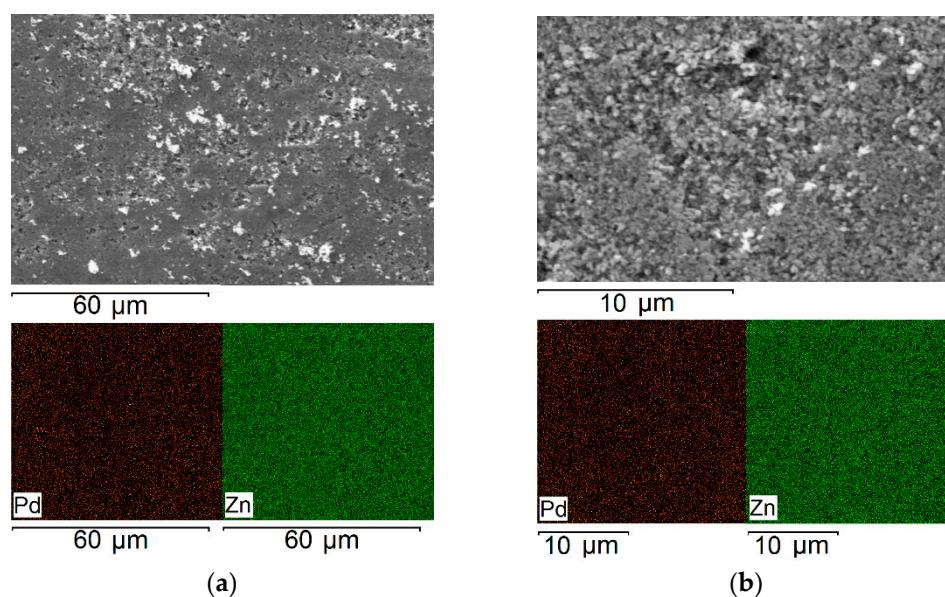
Figure 2. SEM and EDX mapping images of Pd and Zn from the 0.5%Pd/ZnO (**a**) and 0.5%Pd-PVP/ZnO (**b**) catalysts.

The X-ray powder diffraction (XRD) patterns of the 0.5%Pd/ZnO and 0.5%Pd-PVP/ZnO catalysts are shown in Figure 3. The characteristic peaks at 37.0°, 40.1°, 42.3°, 55.7°, 66.7°, 74.5°, 78.9°, 80.8°, 82.3°, 86.8°, and 92.5° corresponding to the [100], [002], [101], [102], [110], [103], [200], [112], [201], [004], and [202] planes of the ZnO wurtzite structure (JCPDS (Joint Committee on Powder Diffraction Standards) card no. 79-0206) [30] were observed in the XRD pattern of the 0.5%Pd/ZnO catalyst.

The XRD pattern of the 0.5%Pd-PVP/ZnO catalyst was nearly the same as before the modification with the polymer. However, a new broad peak at 23.4° appears, which probably corresponds to the amorphous phase of the semi-crystalline PVP [31]. Diffraction peaks related to the palladium species (Pd or PdO) were not detected in both samples which can be explained by low Pd loading and small particle sizes [32].

The presence of the polymer in the 0.5%Pd-PVP/ZnO catalyst was also confirmed by the standardized BET method (Table 2). Adsorption of the PVP on the zinc oxide led to the formation of a PVP/ZnO composite with a decreased surface area due to the covering of the surface of the ZnO with the polymer's organic shell and the blockage of micropores in the inorganic material after modification [33–35]. For the same reason, the 0.5%Pd/ZnO catalyst demonstrated a slightly lower surface area compared with that of the ZnO. On the contrary, the surface area of the 0.5%Pd-PVP/ZnO catalyst was higher than that of the PVP/ZnO composite. This is probably due to a decrease in the surface coverage of the ZnO particles by the polymer shell caused by the interaction of the N-C=O groups of PVP with the Pd species (changing the orientation of the polymer functional groups from

ZnO to Pd). The surface area of the 0.5%Pd-PVP/ZnO catalyst was lower than that of the 0.5%Pd/ZnO catalyst. Despite this, the 0.5%Pd-PVP/ZnO catalyst can be effective in liquid-phase hydrogenation due to the good swelling ability of the PVP polymer shell in ethanol (solvent used hydrogenation process) making the Pd particles more accessible for reactants [36].
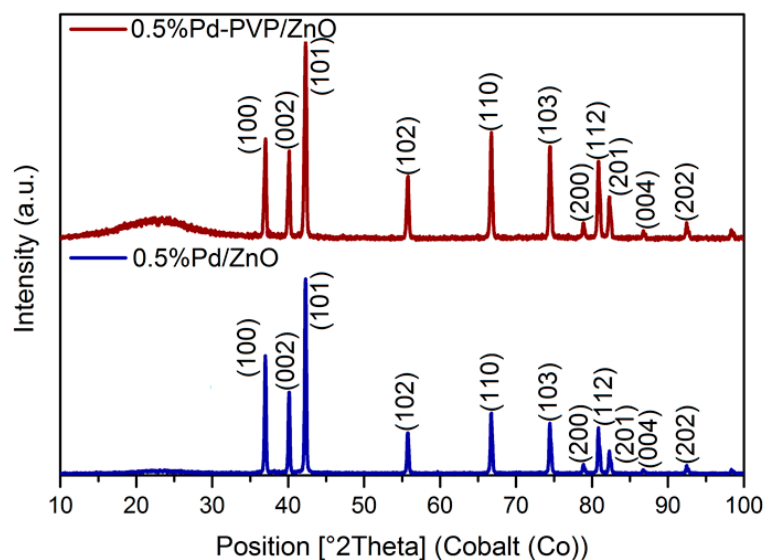

Figure 3. XRD of the 0.5%Pd/ZnO and 0.5%Pd-PVP/ZnO catalysts.

The interactions between the components of the catalysts were studied by infrared spectroscopy (IRS) (Figure 4). PVP shows the characteristic band at 1683 cm^{-1}, corresponding to the pyrrolidone C=O group. Other important bands at 1294 and 1015 cm^{-1} have been attributed to N–C stretching [37,38]. The shifting of the absorption bands of the -C=O and C-N groups in the IR spectra of the catalyst, compared to the same bands in the PVP, Pd-PVP, or PVP/ZnO (Figure 4, spectra 1 to 4), confirms the formation of chemisorbed polymer–metal complexes on the zinc oxide surface.
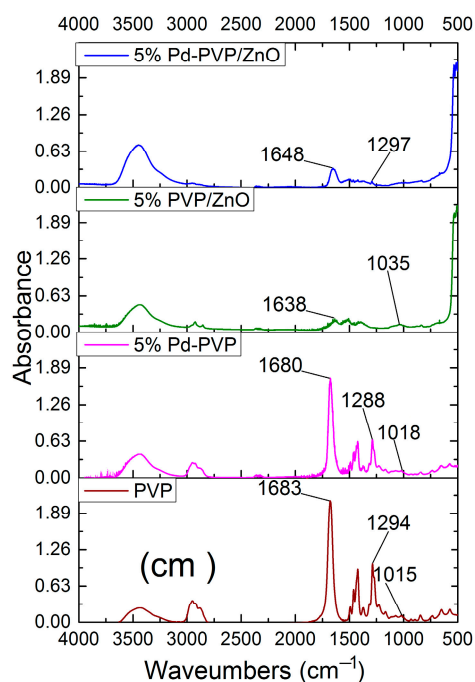

Figure 4. IR spectra of the PVP, Pd/PVP, PVP/ZnO, and 0.5%Pd-PVP/ZnO samples.

The study of the Pd/ZnO and Pd-PVP/ZnO catalysts by transmission electron microscopy (TEM) showed the formation of active phase nanoparticles evenly distributed on a support surface (Figure 5), which is consistent with EDX mapping image data (Figure 2).
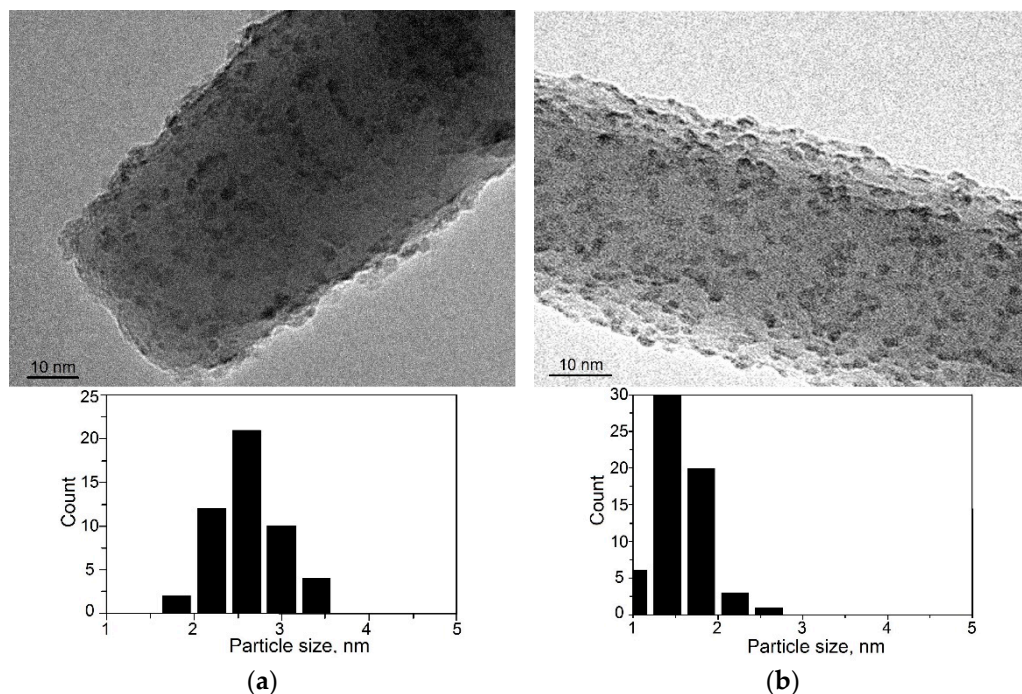

(**a**)   (**b**)

Figure 5. TEM images of the 1%Pd/ZnO (**a**) and 1%Pd-PVP/ZnO (**b**) catalysts and the Pd particle size distribution.

At first sight, nanoparticles seem to be near the same size in both samples. However, a more detailed analysis of the TEM images showed that the PVP-modified catalyst demonstrated smaller mean particle sizes (~1.8 nm) compared with those of the Pd/ZnO (~2.8 nm), confirming the stabilization role of the polymer shell [39].

The lines of zinc, oxygen, carbon, and palladium were detected in the survey X-ray photoelectron spectrum (XPS) of the 0.5%Pd-PVP/ZnO catalyst (Figure 6a), confirming the presence of both polymer and palladium on the ZnO surface.
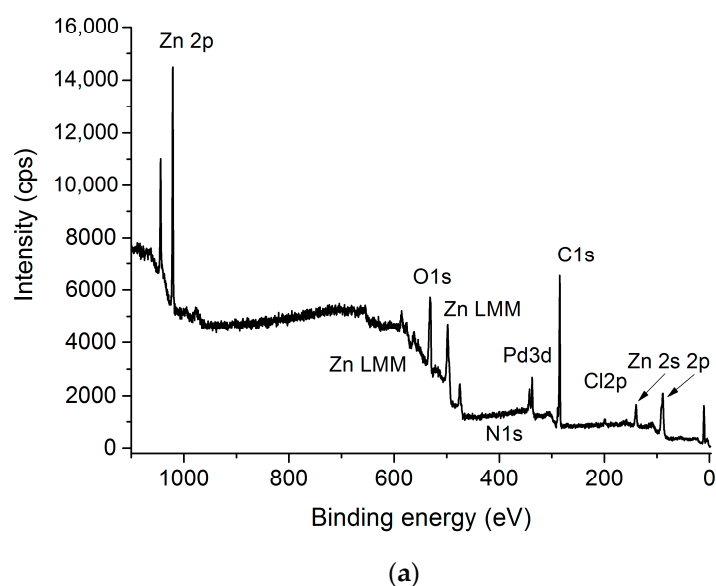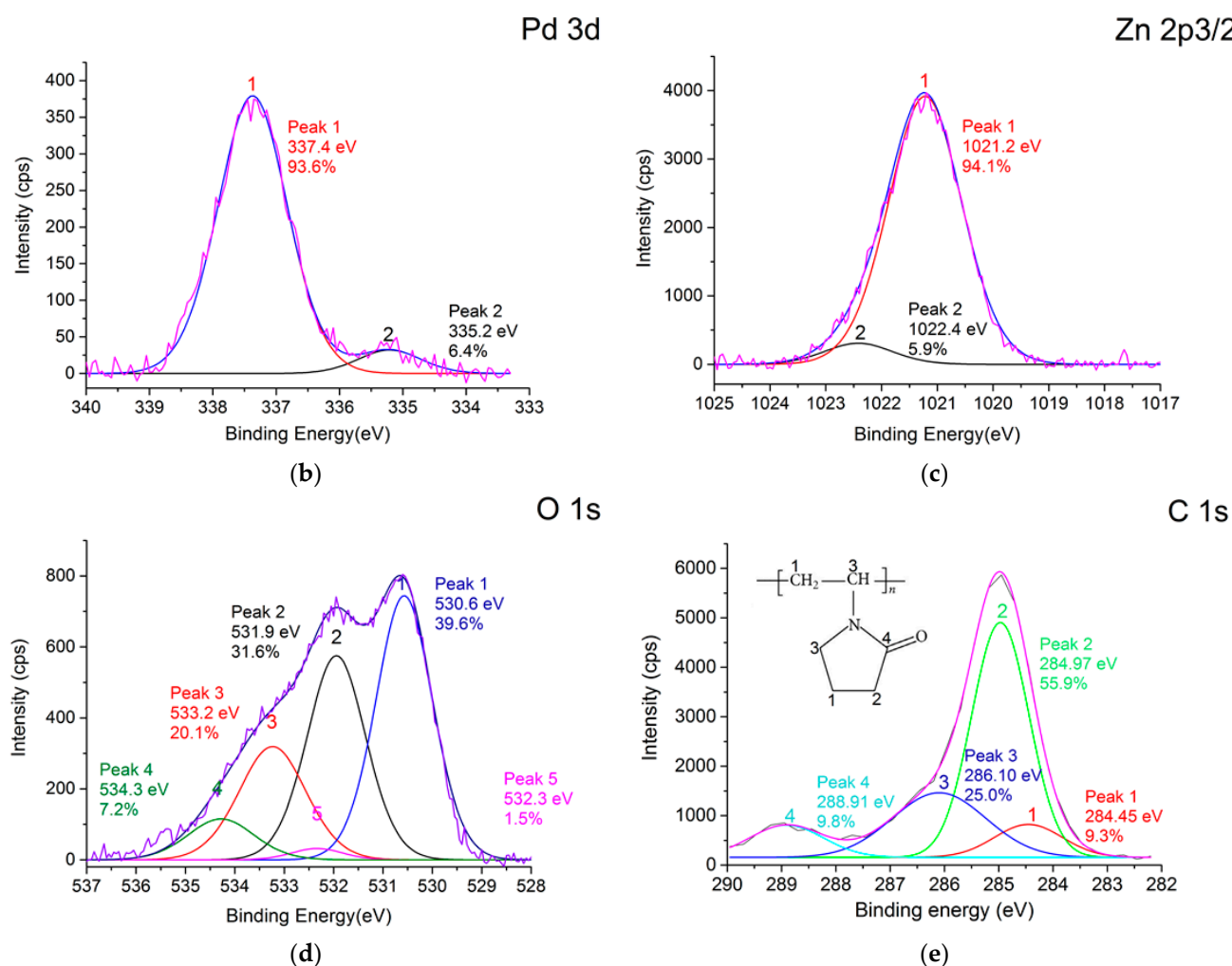

(**a**)

Figure 6. *Cont.*

Figure 6. The XPS results in data for the 0.5%Pd-PVP/ZnO catalyst: survey XPS spectrum (**a**) and curve-fitted XPS spectra of the Pd (3d) (**b**), Zn (2p3/2) (**c**), O (1s) (**d**) and C (1s) (**e**) regions.

According to XPS data, palladium in the 0.5%Pd-PVP/ZnO catalyst was predominantly in the oxidized state, with the Pd 3d(5/2) peak at ~337.4 eV. A small shoulder at ~335.2 eV was observed, indicating the presence of the zero-valent palladium (Figure 6b) [40]. A small amount of Pd^0 was probably caused by the reduction of Pd^{2+} with electrons formed on the semiconductor support surface under the visible light action [41]. The predomination of palladium in an oxidized state in the catalyst requires its reduction before use in a hydrogenation process. According to our prior work [16] palladium can be completely reduced to a zero-valent state after the treatment of a catalyst with molecular hydrogen in a reactor at 40 °C.

The deconvolution of the Zn (2p3/2) peak is shown in Figure 6c. The components observed at ~1021.2 eV and ~1022.4 eV were assigned to Zn^{2+} ions in a ZnO crystal lattice and to the Zn–OH bond, respectively [42]. The peak at ~1022.4 eV can also be assigned to Zn^{2+} ions in the ZnO bonded to the oxygen atom of the polymer.

The XPS spectrum of the O (1s) region presents an asymmetric peak, indicating the presence of different oxygen species with some overlapping with the Pd (3p) line. The curve was fitted to five distinct GL components (1, 2, 3, 4, and 5, as shown in Figure 6d). Peak 1 centered at 530.6 eV is attributed to O^{2-} ions in the Zn-O bonding of the wurtzite structure of Zn^{2+}, whereas peaks 2 and 4 at 531.9 eV and 533.2 eV, respectively, are typically related to the weak bonds of oxygen on the surface, such as the OH groups [43]. Peak 5 centered at 534.3 eV is attributed to Pd (3p) in an oxidized (+2) state [44]. It should be noted

that peaks from oxygen (1s) in PdO and Pd (3p) in a zero-valence state could be overlapped by peaks 1 and 2 [44].

Peak 3 centered at 532.3 eV can be assigned to the carboxyl (C=O) oxygen in the PVP repeated unit, which shifted toward higher binding energy, in contrast to the O (1s) peak from carboxyl (C=O) oxygen (531.3 eV) in pure PVP [45].

The C (1s) peak (Figure 6e) could be de-convoluted into four peaks at 284.5, 285.0, 286.1, and 288.9 eV, which originate from different carbon atoms from 1 to 4, respectively, in the PVP molecules (see the inset in Figure 6e) [45]. The peak (288.9 eV) assigned to carboxyl (C=O) carbon of PVP is shifted towards higher binding energy, in contrast to the C (1s) peak from carboxyl (C=O) carbon (288.1 eV) in pure PVP [38]. The positive shifts of C (1s) and O (1s) peaks from the carboxyl (C=O) group of PVP are consistent with IR spectroscopy data and indicates the interaction between the N-C=O group of the polymer with Pd species.

Thus, the characterization of Pd-PVP/ZnO catalysts using complex physical methods indicate that successive adsorption of PVP and palladium ions on ZnO lead to the formation of immobilized Pd^{2+}-PVP complex uniformly distributed on the support surface. In addition, the coordination of the N-C=O group of PVP to Pd species promotes the formation of smaller particles.

2.2. Hydrogenation of Alkynols

2.2.1. Hydrogenation of 3,7,11-Trimethyldodecyn-1-ol-3 (C_{15}-yn)

In order to study the polymer effect on the activity, selectivity, and stability of palladium catalyst supported on zinc oxide, the synthesized 1%Pd-PVP/ZnO and 1%Pd/ZnO systems were tested in the hydrogenation of 3,7,11-trimethyldodecyn-1-ol-3 (C_{15}-yn) with a reaction at 40 °C, and an atmospheric hydrogen pressure with ethanol as a solvent.

Hydrogenation of 3,7,11-trimethyldodecyn-1-ol-3 on catalysts was carried out with the formation of an ethylene derivative and its subsequent transformation into saturated alcohol (Scheme 1).
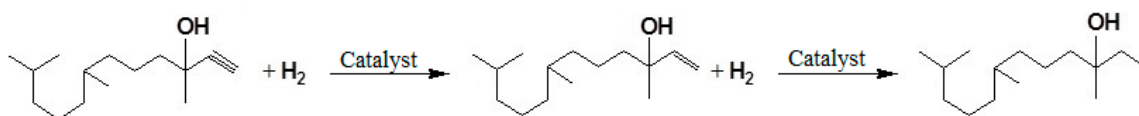
Scheme 1. Hydrogenation of 3,7,11-trimethyldodecyn-1-ol-3.

The activity of catalysts was evaluated by measuring the hydrogen uptake as a function of time. A polymer-containing catalyst demonstrates significantly higher activity compared to unmodified systems. The semi-hydrogenation point (100 mL) over 1%Pd-PVP/ZnO occurs after the first minute of the reaction, whereas with 1%Pd/ZnO this value is reached after twelve minutes (Figure 7a). The hydrogenation rate of acetylene alcohol calculated from data on hydrogen sorption over 1%Pd-PVP/ZnO reaches its maximum at the first minute ($W = 70.0–10^{-6}$ mol/s) and then sharply decreases (Figure 7b). The process on 1%Pd/ZnO (Figure 7b) runs almost 10 times slower ($W = 7.2–10^{-6}$ mol/s). Thus, the introduction of polymer into the catalyst composition leads to an increase in the C_{15} acetylene alcohol hydrogenation rate. This can be explained by the stabilization of palladium particles by polymer as well as by the good swelling ability of the polymer layer in the reaction medium, providing improved access of the long-chain substrate to the active centers of the catalyst.
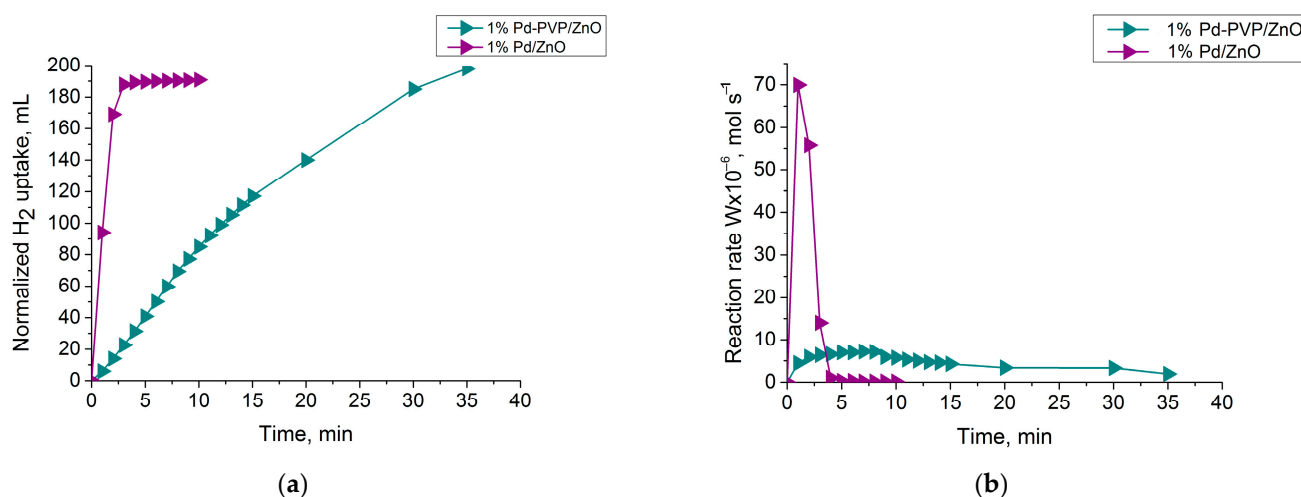
Figure 7. Kinetics of the hydrogen uptake (**a**) and change in reaction rate (**b**) on 1%Pd-PVP/ZnO and 1%Pd/ZnO catalysts during the hydrogenation of 3,7,11-trimethyldodecyn-1-ol-3 to 3,7,11-trimethyldodecen-1-ol-3 and 3,7,11-trimethyldodecan-1-ol-3. Reaction conditions: T = 40 °C, P_{H2} = 1 atm, m_{cat} = 0.05 g, solvent C_2H_5OH 0.25 mL, and $C_{alkynol}$ = 0.09 mol/L.

Polymer modification also leads to an increase in selectivity. According to chromatographic analysis, the maximum yield of 3,7,11-trimethyldodecen-1-ol-3 (C_{15}-en) on 1%Pd-PVP/ZnO was observed at the first minute of the reaction and was 90.4%, which corresponds to the 98% selectivity for C_{15}-en at a substrate conversion of 92.2% (Figure 8a). In the case of the 1%Pd/ZnO catalyst, the maximum yield of C_{15}-en was obtained at the twelfth minute and was 81.8%, which corresponds to the 91% selectivity for C_{15}-en at the C_{15}-yn conversion of 90.0% (Figure 8b).

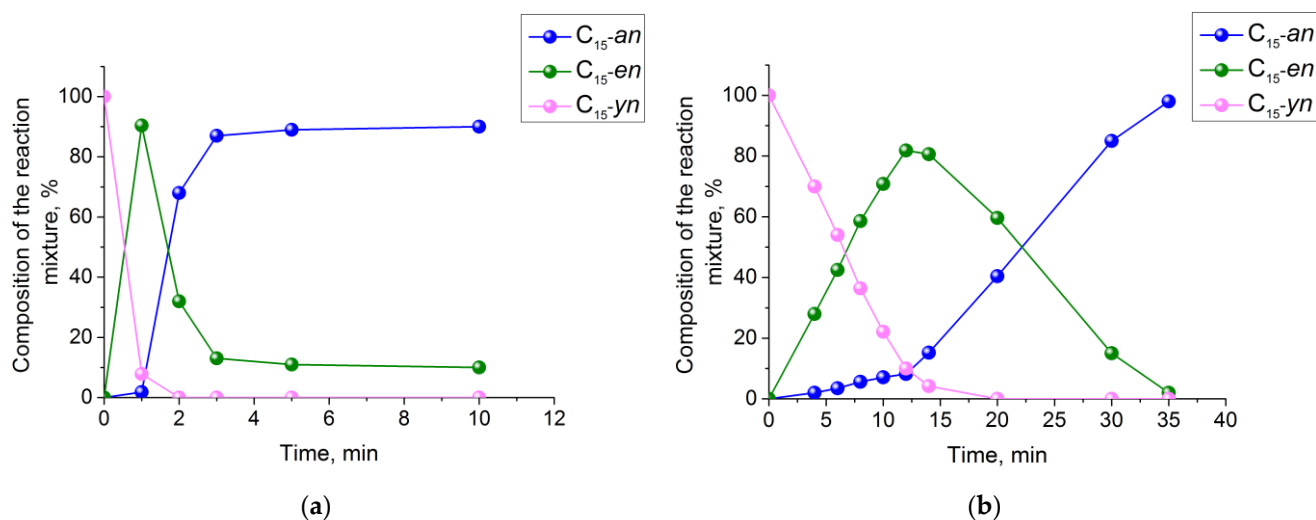**Figure 8.** Changes in the composition of the reaction mixture during the hydrogenation of 3,7,11-trimethyldodecyn-1-ol-3 (C_{15}-yn) to 3,7,11-trimethyldodecen-1-ol-3 (C_{15}-en) and 3,7,11-trimethyldodecan-1-ol-3 (C_{15}-an) in the presence of 1%Pd-PVP/ZnO (**a**) and 1%Pd/ZnO (**b**). Reaction conditions: T = 40 °C, P_{H2} = 1 atm, m_{cat} = 0.05 g, solvent C_2H_5OH 0.25 mL, and $C_{alkynol}$ = 0.09 mol/L.

The stability of the 1%Pd/ZnO and 1%Pd-PVP/ZnO catalysts was studied by the hydrogenation of successive portions of C_{15} acetylene alcohol on one sample of the catalyst (Figure 9). It was shown that both catalysts can be reused for at least 21 runs without degradation in catalytic activity. Further, the activity of catalysts was decreased with each subsequent run. Less stability showed in the 1%Pd/ZnO catalyst, which lost its activity

after 28 runs. The 1%Pd-PVP/ZnO catalyst exhibited much better stability. Sixty-three portions or 73.08 mL of acetylene alcohol were hydrogenated on 0.05 g of this catalyst, which corresponds to 62,000 catalytic cycles on 1 metal atom in terms of turnover number (TON). Improved catalytic properties of the PVP-modified catalyst can be explained by the stabilization role of the polymer, leading to the formation of smaller Pd particles [39] and the prevention of their leaching from the support surface. This was confirmed in a parallel stability experiment. After 30 runs, the catalyst was separated from the reaction mixture, washed with water, dried, and analyzed by EDX elemental analysis. The palladium content in the reused catalyst (0.98 wt.%) was near the same as in the initial one (0.92 wt.%). In addition, hydrogenation of the C_{15} acetylene alcohol did not proceed in the filtrate but was obtained by the separation of the reused catalyst (30 runs) from the catalysate (mixture of catalyst and reaction products). The Pd content in the spent 1%Pd-PVP/ZnO catalyst (after 63 runs) was 0.83 wt.%. This suggests that the deactivation of the catalyst was not associated with the leaching of the Pd species from the support surface. In our prior studies [15,36], it was shown that the accumulation of reaction products on such catalyst surface types led to a shrinking of the polymer shell, agglomeration of polymer-protected Pd particles, and a decrease in their activity. In this regard, the increased lifetime of the 1%Pd-PVP/ZnO catalyst can also be explained by the good swelling ability of the PVP shell in the reaction mixture containing ethanol, providing access to the substrate of the active centers [15]. Thus, the 1%Pd-PVP/ZnO catalyst combines the advantages of both homogeneous and heterogeneous catalysts.
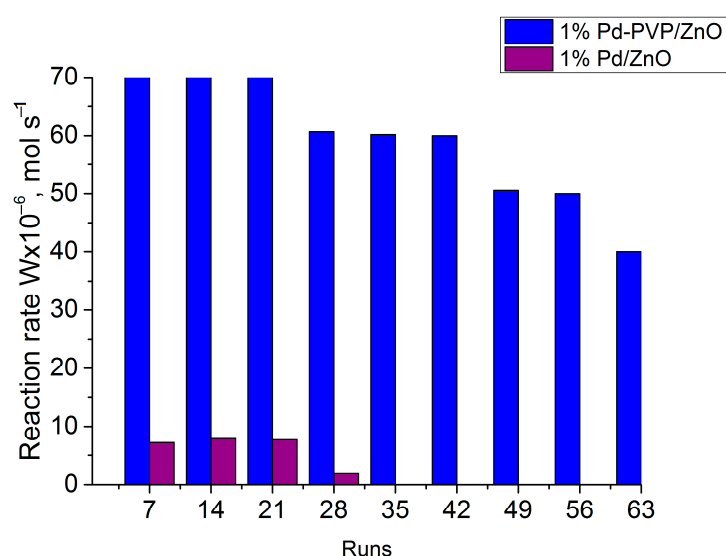

Figure 9. Consecutive hydrogenation of 3,7,11-trimethyldodecyn-1-ol-3 portions in the presence of 1%Pd-PVP/ZnO and 1%Pd/ZnO. Reaction conditions: T = 40 °C, P_{H2} = 1 atm, m_{cat} = 0.05 g, solvent C_2H_5OH 0.25 mL, and $C_{alkynol}$ = 0.09 mol/L.

The efficiency of the catalyst system is considered the main characteristic in determining technical and economic indicators of catalyst production rather than its cost. However, it is reasonable to consider ways of reducing the catalyst cost while maintaining its efficiency. In this work, available and inexpensive reagents, polyvinylpyrrolidone and zinc oxide, were used for the synthesis of the 1%Pd/ZnO and 1%Pd-PVP/ZnO catalysts. Palladium, which belongs to the platinum group of metals, makes the main contribution to the cost of the catalytic system. Analysis of the results obtained for the hydrogenation of the C_{15}-yn acetylene alcohol on the studied catalysts showed that modification with polyvinylpyrrolidone increases the activity, selectivity, and stability of the 1%Pd/ZnO catalyst (Table 3) which gives additional opportunities for noble metal content reduction.

Table 3. Results of the hydrogenation of 3,7,11-trimethyldodecyn-1-ol-3 in ethanol on Pd catalysts.

Catalyst	$W_{max} \cdot 10^{-6}$ (mol s^{-1}) *	TOF s^{-1}	TON	$S_{C=C}$,%
1%Pd/ZnO	7.2	1.5	17,000	91
1%Pd-PVP/ZnO	70.0	15.0	62,000	98
0.5%Pd-PVP/ZnO	67.8	28.9	21,100	98
0.25%Pd-PVP/ZnO	21.0	18.0	42,300	98

* Maximum rate of reaction ($W_{max} \cdot 10^{-6}$) in mol s^{-1}.

In order to obtain catalysts with a lower content of active components, the Pd-PVP/ZnO systems containing 0.5 and 0.25% palladium were prepared and tested. A decrease in the active component content from 1 to 0.5% leads to an increase in the activity of the catalyst. At further reduction of palladium content in the catalyst, the process rate decreases sharply, almost threefold (Table 3).

In terms of specific activity, expressed in turnover frequency (TOF) units, a decrease in the palladium percentage leads to an increase in the efficiency of catalysts. The catalyst with a palladium content of 0.5% is as selective and even twice as active as the catalyst with a metal content of 1%. That means that a reduction of the active phase content without deterioration and in some cases with an improvement of the catalyst characteristics and its significant cheapening is possible since zinc oxide and polyvinylpyrrolidone are available and inexpensive components. Reducing the content of the active phase does not affect the selectivity of the process, which is 98% in all cases (Table 3). A sharp decrease in activity is observed on the catalyst containing 0.25% palladium, although the stability of the 0.25%Pd-PVP/ZnO catalyst is higher than that containing 0.5%Pd (Table 3). The polymer-free palladium catalyst exhibits poor catalytic properties.

The values of selectivity to alkenol (S_{en}) and the reaction rate in terms of TOF were comparable with those indicated for other known Pd-catalysts studied in the hydrogenation of various alkynols: Lindlar catalyst (substrate-2-methyl-3-butyn-2-ol, S_{en} = 93%, TOF = 2.2 s^{-1}) [46], Pd-In/In$_2$O$_3$-250 (substrate-2-methyl-3-butyn-2-ol, S_{en} = 98%, TOF = 12.9 s^{-1}) [46], Pd-ZnO-400 (2-butyne-1,4-diol, S_{en} = 92.6%, TOF =1.18 s^{-1}) [47], Pd/Al$_2$O$_3$/SMF (substrate-2-butyne-1,4-diol, S_{en} = 97.1%, TOF = 24.5 s^{-1}) [48], Pd/ZnO/SMF (substrat -2-butyne-1,4-diol, S_{en} = 99%, and TOF = 10.8 s^{-1}) [48]. Thus, it is possible to reduce the amount of expensive palladium in catalysts to 0.5% in order to reduce their cost.

2.2.2. Hydrogenation of 2-Hexyn-1-ol

The 0.5%Pd-PVP/ZnO catalyst showing high catalytic activity in the reaction of hydrogenation of complex acetylene alcohol C$_{15}$-yn was tested in the stereoselective hydrogenation of short-chain 2-hexyn-1-ol under similar experimental conditions. In all cases, the simultaneous formation of three reaction products was observed: cis-2-hexen-1-ol, trans-2-hexen-1-ol, and hexan-1-ol (Scheme 2).
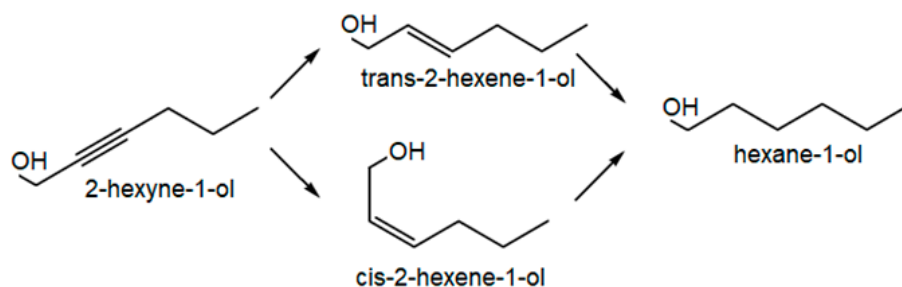
Scheme 2. Hydrogenation of 2-hexyn-1-ol.

For comparison, hydrogenation was performed on a 0.5%Pd/ZnO polymer-free catalyst.

At hydrogenation of 2-hexyn-1-ol on the 0.5%Pd-PVP/ZnO and 0.5%Pd/ZnO catalysts, the half-hydrogenation point (50 mL) was reached after 11 and 14 min of the

process, respectively (Figure 10a). The hydrogenation rate of 2-hexyn-1-ol calculated from hydrogen absorption data is shown in Figure 10b. Maximum values of the substrate hydrogenation rate for the 0.5%Pd-PVP/ZnO and 0.5%Pd/ZnO catalysts were $8.1–10^{-6}$ and $5.4–10^{-6}$ mol/s, respectively.
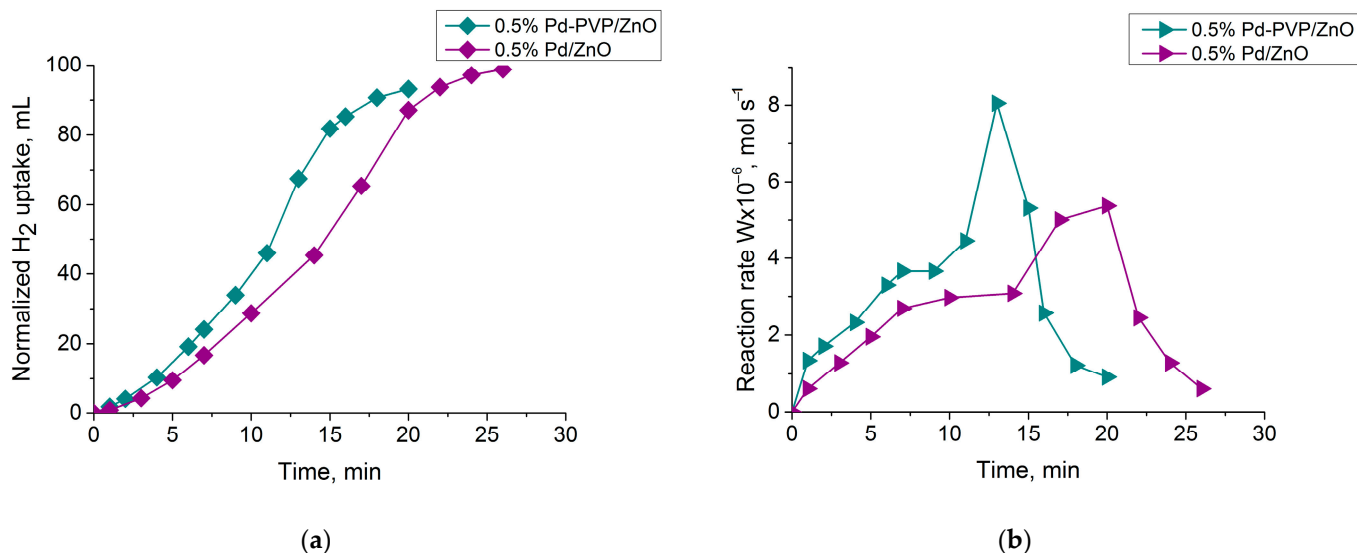

Figure 10. Kinetics of the hydrogen uptake (**a**) and change in reaction rate (**b**) on the 0.5%Pd-PVP/ZnO and 0.5%Pd/ZnO catalysts during the hydrogenation of 2-hexyn-1-ol to cis-2-hexen-1-ol, trans-2-hexen-1-ol and hexan-1-ol. Reaction conditions: T = 40 °C, P_{H2} = 1 atm, m_{cat} = 0.05 g, solvent C_2H_5OH 0.25 mL, and $C_{alkynol}$ = 0.09 mol/L.

According to chromatographic analysis, the maximum yield of cis-hexen-2-ol on the 0.5%Pd-PVP/ZnO catalyst is observed at the eleventh minute and is 87.2%, with 91.2% conversion of 2-hexyn-1-ol. This corresponds to 95.6% cis-alkene selectivity (Figure 11a).
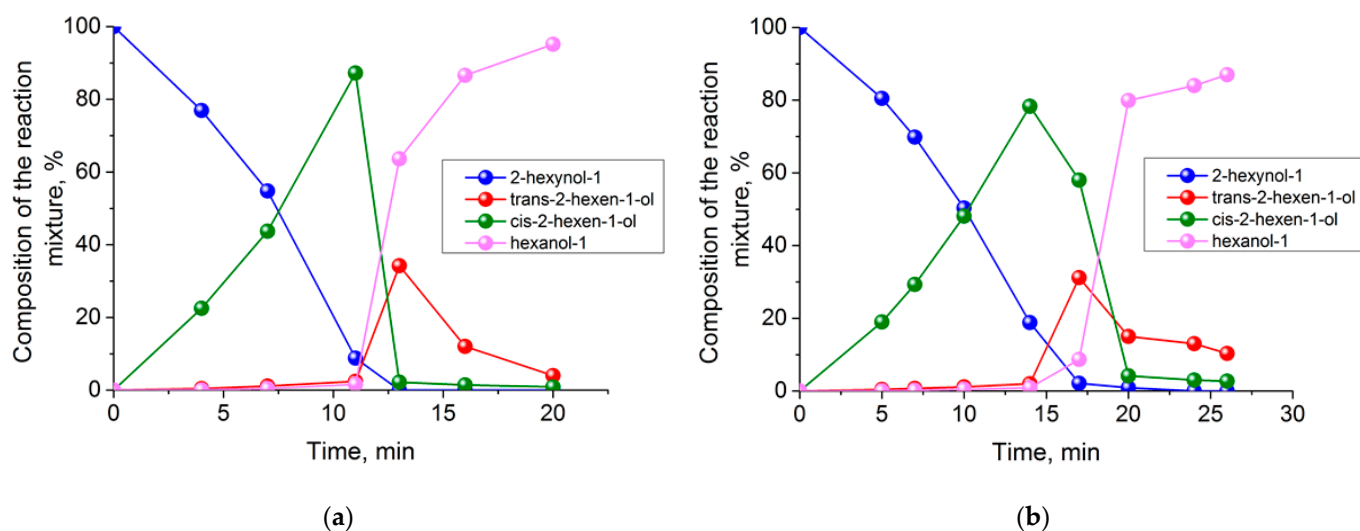

Figure 11. Changes in the composition of the reaction mixture during the hydrogenation of 2-hexyn-1-ol to cis-2-hexen-1-ol, trans-2-hexen-1-ol and hexan-1-ol in the presence of 0.5%Pd-PVP/ZnO (**a**) and 0.5%Pd/ZnO (**b**). Reaction conditions: T = 40 °C, P_{H2} = 1 atm, m_{cat} = 0.05 g, solvent C_2H_5OH 0.25 mL, and $C_{alkynol}$ = 0.09 mol/L.

The maximum yield of cis-hexen-2-ol on the polymer-free catalyst occurred at the fourteenth minute and was 78.3%, which corresponds to 96.4% selectivity for cis-2-hexen-1-ol at 81.2% conversion of 2-hexyn-1-ol.

It should be noted that both catalysts show close stereoselectivity for cis-hexen-1-ol (Table 4).

Table 4. Results of hydrogenation of 2-hexynol-1 in ethanol on the 0.5% palladium catalysts.

Catalyst	$W_{max} \cdot 10^{-6}$ (mol s^{-1}) *	$S_{cis-hexen-1-ol}$,%
Pd/ZnO	5.4	96.4
Pd-PVP/ZnO	8.1	95.6

* Maximum rate of reaction ($W_{max} \cdot 10^{-6}$) in mol s^{-1}.

According to the hydrogenation of cis-2-hexyn-1-ol, a correlation with results obtained during the hydrogenation of 3,7,11-trimethyldodecyn-1-ol-3 was observed. Thus, the values of the hydrogenation reaction rate and the yield of the target product (3,7,11-trimethyldodecen-1-ol-3, cis-2-hexen-1-ol) in the presence of PVP-modified palladium catalyst are approximately 10% higher than those of non-modified palladium catalyst.

3. Materials and Methods

3.1. Materials

The 3,7,11-trimethyldodecyn-1-ol-3 (HCCCOH(CH$_3$)(CH$_2$)$_3$CH(CH$_3$)(CH$_2$)$_3$CH(CH$_3$)$_2$–C$_{15}$-yn) were purchased from Angene International Limited (Nanjing, China) and 2-hexyn-1-ol (97%, Sigma-Aldrich, St. Louis, MO, USA). Ethanol (reagent grade, Sigma-Aldrich, St. Louis, MO, USA), palladium chloride (PdCl$_2$, 59–60% Pd, Sigma-Aldrich, St. Louis, MO, USA), potassium chloride (KCl, reagent grade, St. Louis, MO, USA), polyvinylpyrrolidone (PVP, Mw 40,000, Sigma-Aldrich, St. Louis, MO, USA) were used without additional purification. Zinc oxide (chemically pure, Sigma-Aldrich, St. Louis, MO, USA) was used as an inorganic support.

3.2. Preparation of K$_2$PdCl$_4$ Precursor Solution

The 0.019 M K$_2$PdCl$_4$ precursor solution was obtained by grinding 168.4 mg of PdCl$_2$ and 155.7 mg of KCl in an agate mortar, followed by dissolving the resulting potassium tetrachloropalladate(II) in 50 mL of distilled water at 70 °C and magnetic stirring for 2 h.

3.3. Synthesis of Catalysts

A 5 mL solution of 0.5–1.9 × 10^{-2} M PVP (0.0017–0.0067 g in 5 mL of water) was added dropwise to a suspension of zinc oxide (1 g) in water (15 mL) at room temperature, and the resulting mixture was stirred for 2 h. Then, 5 mL of a 0.5–1.9 × 10^{-2} M K$_2$PdCl$_4$ solution was added dropwise and stirred for 3 h. The concentration of PVP and palladium salt solutions (0.5 × 10^{-2}, 0.9 × 10^{-2}, and 1.9 × 10^{-2} M) were taken from a calculation for the preparation of catalysts with 0.25, 0.5, and 1% palladium content and [Pd:PVP] molar ratio = 1:1. The resulting catalyst was kept in the mother liquor for 12–15 h. Thereafter, it was washed with water and then dried in air. The completeness of palladium immobilization was controlled by photoelectric colorimetry. For comparison, similar Pd/ZnO catalysts were prepared using the same procedure except that the polymer was added.

3.4. Characterization of Catalysts

The palladium content in the catalysts was preliminarily evaluated based on the change in metal ion concentration in mother liquor before and after immobilization of PdCl$_4^{2-}$ on polymer-modified zinc oxide. The palladium content in mother liquors was determined from photoelectric colorimetry data, which were obtained on an SF-2000 UV/Vis spectrophotometer (OKB Spectr, Saint-Petersburg, Russia), based on calibration curves constructed at the wavelength λ = 425 nm.

The powder X-ray diffraction (XRD) patterns were obtained with DRON-4-0.7 X-ray diffractometer (Bourevestnik, Russia) using cobalt monochromatized Co-Kα radiation (λ = 0.179 nm).

The measurement of specific surface area and pore size distribution was carried out by a low-temperature N_2 adsorption–desorption technique using Accusorb equipment (Micromeritics, Norcross, GA, USA).

Fourier transform infrared (FTIR) spectra of catalyst samples were obtained using a Nicolet iS5 (Thermo Scientific, Waltham, MA, USA) in the 4000–400 cm^{-1} region. Pellets for infrared analysis were obtained by grinding a mixture of a 1 mg sample with 100 mg dry KBr, followed by pressing the mixture into a mold.

The transmission and scanning electron microscopy studies were performed on a JEM-2100 transmission electron microscope (Jeol, Tokyo, Japan) with an accelerating voltage of 100 kV and a scanning electron microscope JSM-6610LV with EDX-detector (Jeol, Japan).

The analysis of the catalyst by X-ray photoelectron spectroscopy (XPS) was carried out on a Kratos Axis Ultra DLD photoelectron spectrometer (Kratos Analytical LTD, Manchester, UK).

3.5. Hydrogenation of Alkynols

Hydrogenation was performed in a thermostatically controlled long-necked glass flask reactor in an ethanol solution (25 mL) at one atmosphere in ambient hydrogen and a temperature of 40 °C, with intensive stirring (600–700 oscillations per minute). The catalyst (0.05 g) was treated preliminarily with hydrogen directly in the reactor for 30 min, with intensive stirring. Then, 2.23 mmol (0.09 mol/L) of a substrate was introduced. The substrate amount was taken based on the uptake of 100–200 mL of hydrogen. The reaction rate was calculated from the hydrogen uptake per unit of time. For this purpose, the volume of uptaken hydrogen was measured at a definite time interval using a burette connected to the reactor.

To determine the selectivity of the main reaction products, samples of the reaction mixture were taken at fixed times with a syringe, and analyzed by gas chromatography. The analysis was carried out on a Khromos GKh1000 chromatograph (Khromos, Russia) with a flame ionization detector in the isothermal regime using a BP21 (FFAP) capillary column with a polar phase (PEG-modified with nitroterephthalate) 50 m in length and 0.32 mm in inside diameter. The column temperature was 90 °C and the injector temperature was 200 °C; helium served as the carrier gas; the injected sample volume was 0.2 μL. The selectivity to styrene was evaluated as the fraction of the target product in the reaction products at a specified degree of conversion.

The stability of the systems was assessed by conducting the hydrogenation on successive portions (2.23–4.46 mmol) of substrate for the same sample of catalyst (0.05 g).

4. Conclusions

In this study, a simple method was proposed for supported palladium catalyst synthesis, which allowed polymer-stabilized palladium nanoparticles uniformly distributed on a zinc oxide surface to be obtained, which was confirmed by XRD, IRS, BET, TEM, etc. methods. It was shown that the modification of a deposited palladium catalyst with polymer significantly affected the catalytic properties of the synthesized Pd-PVP/ZnO system. The 1%Pd-PVP/ZnO catalyst was active (W = 70 × 10^{-6} mol/s), selective for the target product (98%), and stable (TON = 62,000) in the hydrogenation of 3,7,11-trimethyldodecyn-1-ol-3 under mild conditions (40 °C, 0.1 MPa). The high activity of the Pd-PVP/ZnO catalyst was probably due to the stabilization of the palladium nanoparticles by ethanol-soluble PVP, which provided good dispersion of the active phase, as well as the fact that the system swells under the influence of solvent during liquid-phase hydrogenation, which facilitates the access of substrates to the metal-catalyst particles.

In addition, the modification with the polymer was shown to be a promising way to reduce noble metal content in the catalysts without significant loss in their activity and selectivity. The synthesized polymer-modified catalyst with 0.5% palladium was as active and selective as that with 1% palladium, which allowed a reduction of the content of the active phase without deteriorating the catalytic properties of the catalyst.

Testing the 0.5%Pd-PVP/ZnO catalyst in the stereoselective hydrogenation of 2-hexyn-1-ol allows the consideration of this catalyst as promising for the hydrogenation of other acetylene alcohols. As in the case of hydrogenation of complex C_{15-yn} acetylene alcohol, higher values of rate and yield of the target product (higher by almost 10%) were obtained on PVP-containing palladium catalyst compared with unmodified Pd/ZnO catalyst.

References

1. Stoffels, M.A.; Klauck, F.J.R.; Hamadi, T.; Glorius, F.; Leker, J. Technology Trends of Catalysts in Hydrogenation Reactions: A Patent Landscape Analysis. *Adv. Synth. Catal.* **2020**, *362*, 1258–1274. [CrossRef]
2. Yang, C.; Teixeira, A.R.; Shi, Y.; Born, S.C.; Lin, H.; Li Song, Y.; Martin, B.; Schenkel, B.; Lachegurabi, M.P.; Jensen, K.F. Catalytic hydrogenation of N-4-nitrophenyl nicotinamide in a micro-packed bed reactor. *Green Chem.* **2018**, *20*, 886–893. [CrossRef]
3. Mironenko, R.M.; Belskaya, O.B.; Likholobov, V.A. Approaches to the synthesis of Pd/C catalysts with controllable activity and selectivity in hydrogenation reactions. *Catal. Today* **2019**, *357*, 152–165. [CrossRef]
4. Zhao, X.; Chang, Y.; Chen, W.-J.; Wu, Q.; Pan, X.; Chen, K.; Weng, B. Recent Progress in Pd-Based Nanocatalysts for Selective Hydrogenation. *ACS Omega* **2022**, *7*, 17–31. [CrossRef] [PubMed]
5. Bonrath, W.; Medlock, J.; Schutz, J.; Wustenberg, B.; Netscher, T. Hydrogenation in the Vitamins and Fine Chemicals Industry—An Overview. In *Hydrogenation*; Karamé, I., Ed.; IntechOpen: London, UK, 2012; pp. 17–47. [CrossRef]
6. Albuquerque, B.L.; Denicourt-Nowicki, A.; Mériadec, C.; Domingos, J.B.; Roucoux, A. Water soluble polymer–surfactant complexes-stabilized Pd(0) nanocatalysts: Characterization and structure–activity relationships in biphasic hydrogenation of alkenes and α,β-unsaturated ketones. *J. Catal.* **2016**, *340*, 144–153. [CrossRef]
7. Monguchi, Y.; Ichikawa, T.; Sajiki, H. Recent Development of Palladium-Supported Catalysts for Chemoselective Hydrogenation. *Chem. Pharm. Bull.* **2017**, *65*, 2–9. [CrossRef]
8. McMillan, L.; Gilpin, L.F.; Baker, J.; Brennan, C.; Hall, A.; Lundie, D.T.; Lennon, D. The application of a supported palladium catalyst for the hydrogenation of aromatic nitriles. *J. Mol. Catal. A Chem.* **2016**, *411*, 239–246. [CrossRef]
9. Dobrezberger, K.; Bosters, J.; Moser, N.; Yigit, N.; Nagl, A.; Föttinger, K.; Lennon, D.; Rupprechter, G. Hydrogenation on Palladium Nanoparticles Supported by Graphene Nanoplatelets. *J. Phys. Chem. C* **2020**, *124*, 23674–23682. [CrossRef] [PubMed]
10. Xu, S.; Du, J.; Zhou, Q.; Li, H.; Wang, C.; Tang, J. Selective and leaching-resistant palladium catalyst on a porous polymer support for phenol hydrogenation. *J. Colloid Interface Sci.* **2021**, *604*, 876–884. [CrossRef]
11. Liu, Y.; Huang, A.; Chen, J.; Chen, L.; Hua, J. Hydrogenation catalysis of nanosized palladium supported by polymer/silica disupporter. II. Effects of the characteristics of the catalyst on hydrogenation. *J. Appl. Polym. Sci.* **2003**, *89*, 3661–3665. [CrossRef]
12. Lee, S.; Shin, S.-J.; Baek, H.; Choi, Y.; Hyun, K.; Seo, M.; Kim, K.; Koh, D.-Y.; Kim, H.; Choi, M. Dynamic metal-polymer interaction for the design of chemoselective and long-lived hydrogenation catalysts. *Sci. Adv.* **2020**, *6*, eabb7369. [CrossRef] [PubMed]
13. Ródenas, M.; El Haskouri, J.; Ros-Lis, J.V.; Marcos, M.D.; Amorós, P.; Úbeda, M.Á.; Pérez-Pla, F. Highly Active Hydrogenation Catalysts Based on Pd Nanoparticles Dispersed along Hierarchical Porous Silica Covered with Polydopamine as Interfacial Glue. *Catalysts* **2020**, *10*, 449. [CrossRef]
14. Jiang, Y.; Jiang, J.; Gao, Q.; Ruan, M.; Yu, H.; Qi, L. A novel nanoscale catalyst system composed of nanosized Pd catalysts immobilized on Fe_3O_4@SiO_2-PAMAM. *Nanotechnology* **2008**, *19*, 075714. [CrossRef] [PubMed]
15. Zharmagambetova, A.K.; Talgatov, E.T.; Auyezkhanova, A.S.; Tumabayev, N.Z.; Bukharbayeva, F.U. Effect of polyvinylpyrrolidone on the catalytic properties of Pd/γ-Fe_2O_3 in phenylacetylene hydrogenation. *React. Kinet. Mech. Catal.* **2020**, *131*, 153–166. [CrossRef]

16. Zharmagambetova, A.K.; Seitkalieva, K.S.; Talgatov, E.T.; Auezkhanova, A.S.; Dzhardimalieva, G.I.; Pomogailo, A.D. Polymer Modified Supported Palladium Catalysts for the Hydrogenation of Acetylene Compounds. *Kinet. Catal.* **2016**, *57*, 360–367. [CrossRef]

17. Moreno-Marrodan, C.; Liguori, F.; Barbaro, P.; Sawa, H. Continuous flow catalytic partial hydrogenation of hydrocarbons and alcohols over hybrid Pd/ZrO$_2$/PVA wall reactors. *Appl. Catal. A Gen.* **2018**, *558*, 34–43. [CrossRef]

18. Karakhanov, E.A.; Zolotukhina, A.V.; Ivanov, A.O.; Maximov, A.L. Dendrimer-Encapsulated Pd Nanoparticles, Immobilized in Silica Pores, as Catalysts for Selective Hydrogenation of Unsaturated Compounds. *ChemistryOpen* **2019**, *8*, 358–381. [CrossRef]

19. Chen, X.; Shi, C.; Liang, C. Highly selective catalysts for the hydrogenation of alkynols: A review. *Chin. J. Catal.* **2021**, *42*, 2105–2121. [CrossRef]

20. Zhang, M.; Yang, Y.; Li, C.; Liu, Q.; Williams, C.T.; Liang, C. PVP–Pd@ZIF-8 as highly efficient and stable catalysts for selective hydrogenation of 1,4-butynediol. *Catal. Sci. Technol.* **2014**, *4*, 329–332. [CrossRef]

21. Pomogailo, A.D.; Dzhardimalieva, G.I. Hybrid Polymer-Immobilized Nanosized Pd Catalysts for Hydrogenation Reaction Obtained via Frontal Polymerization. *J. Catal.* **2012**, *2013*, 1–12. [CrossRef]

22. Mirzoeva, E.S.; Bronstein, L.; Valetsky, P.M.; Sulman, E.M. Catalytic hydrogenation properties of Pd- and Rh-containing polymers immobilized on Al$_2$O$_3$. *React. Polym.* **1995**, *24*, 243–250. [CrossRef]

23. Mostafa, M.M.M.; Saleh, T.S.; Bawaked, S.M.; Alghamdi, K.S.; Narasimharao, K. Efficient and Eco-Friendly Perspectives for C-H Arylation of Benzothiazole Utilizing Pd Nanoparticle-Decorated Chitosan. *Catalysts* **2022**, *12*, 1000. [CrossRef]

24. Albano, G.; Petri, A.; Aronica, L.A. Palladium Supported on Bioinspired Materials as Catalysts for C–C Coupling Reactions. *Catalysts* **2023**, *13*, 210. [CrossRef]

25. Nikoshvili, L.Z.; Tikhonov, B.B.; Ivanov, P.E.; Stadolnikova, P.Y.; Sulman, M.G.; Matveeva, V.G. Recent Progress in Chitosan-Containing Composite Materials for Sustainable Approaches to Adsorption and Catalysis. *Catalysts* **2023**, *13*, 367. [CrossRef]

26. Zharmagambetova, A.K.; Auyezkhanova, A.S.; Talgatov, E.T.; Jumekeyeva, A.I. Chitosan-Modified Palladium Catalysts in Hydrogenation of n-Hex-2-yne. *Theor. Exp. Chem.* **2021**, *57*, 371–376. [CrossRef]

27. Zharmagambetova, A.K.; Auyezkhanova, A.S.; Talgatov, E.T.; Akhmetova, S.N.; Tumabayev, N.Z.; Rafikova, K.S.; Talgatov, E.T.; Akhmetova, S.N. Polysaccharide-Stabilized Nanocatalysts in Hydrogenation of Phenylacetylene. *Theor. Exp. Chem.* **2020**, *56*, 39–45. [CrossRef]

28. Zharmagambetova, A.; Auyezkhanova, A.; Talgatov, E.; Jumekeyeva, A.; Buharbayeva, F.; Akhmetova, S.; Myltykbayeva, Z.; Lopez Nieto, J.M. Synthesis of polymer protected Pd-Ag/ZnO catalysts for phenylacetylene hydrogenation. *J. Nanoparticle Res.* **2022**, *24*, 1–17. [CrossRef]

29. Zhong, R.; Yang, J.; Hu, Z.; Xu, B. Removal of Residual Polyvinylpyrrolidone (PVP) from Au Nanoparticles Immobilized in SiO$_2$ by Ultraviolet-Ozone Treatment. *ACS Appl. Nano Mater.* **2019**, *2*, 5720–5729. [CrossRef]

30. Devi, P.G.; Velu, A.S. Synthesis, structural and optical properties of pure ZnO and Co doped ZnO nanoparticles prepared by the co-precipitation method. *J. Theor. Appl. Phys.* **2016**, *10*, 233–240. [CrossRef]

31. Vijaya, N.; Selvasekarapandian, S.; Nithya, H.; Sanjeeviraja, C. Proton Conducting Polymer Electrolyte based on Poly (N-vinyl pyrrolidone) Doped with Ammonium Iodide. *Int. J. Electroact. Mater.* **2015**, *3*, 20–27.

32. Reddy, G.K.; Peck, T.C.; Roberts, C.A. "PdO vs. PtO"—The Influence of PGM Oxide Promotion of Co$_3$O$_4$ Spinel on Direct NO Decomposition Activity. *Catalysts* **2019**, *9*, 62. [CrossRef]

33. Talgatov, E.T.; Auezkhanova, A.S.; Kapysheva, U.N.; Bakhtiyrova, S.K.; Zharmagambetova, A.K. Synthesis and Detoxifying Properties of Pectin-Montmorillonite Composite. *J. Inorg. Organomet. Polym.* **2016**, *26*, 1387–1391. [CrossRef]

34. Cinausero, N.; Azema, N.; Cochez, M.; Ferriol, M.; Essahli, M.; Ganachaud, F.; Lopez-Cuesta, J.-M. Influence of the surface modification of alumina nanoparticles on the thermal stability and fire reaction of PMMA composites. *Polym. Adv. Technol.* **2008**, *19*, 701–709. [CrossRef]

35. Wan Ngah, W.S.; Teong, L.C.; Hanafiah, M.A.K.M. Adsorption of dyes and heavy metal ions by chitosan composites: A review. *Carbohydr. Polym.* **2011**, *83*, 1446–1456. [CrossRef]

36. Zharmagambetova, A.K.; Talgatov, E.T.; Auyezkhanova, A.S.; Tumabayev, N.Z.; Bukharbayeva, F.U. Behavior of Pd-supported catalysts in phenylacetylene hydrogenation: Effect of combined use of polyvinylpyrrolidone and NaOH for magnetic support modification. *Polym. Adv. Technol.* **2021**, *32*, 2735–2743. [CrossRef]

37. Baganizi, D.R.; Nyairo, E.; Duncan, S.A.; Singh, S.R.; Dennis, V.A. Interleukin-10 Conjugation to Carboxylated PVP-Coated Silver Nanoparticles for ImprovedStability and Therapeutic Efficacy. *Nanomaterials* **2017**, *7*, 165. [CrossRef]

38. Mireles, L.K.; Wu, M.-R.; Saadeh, N.; Yahia, L.; Sacher, E. Physicochemical Characterization of Polyvinyl Pyrrolidone: A Tale of Two Polyvinyl Pyrrolidones. *ACS Omega* **2020**, *5*, 30461–30467. [CrossRef]

39. Zharmagambetova, A.K.; Zamanbekova, A.T.; Darmenbayeva, A.S.; Auyezkhanova, A.S.; Jumekeyeva, A.I.; Talgatov, E.T. Effect of Polymers on the Formation of Nanosized Palladium Catalysts and Their Activity and Selectivity in the Hydrogenation of Acetylenic Alcohols. *Theor. Exp. Chem.* **2017**, *53*, 265–269. [CrossRef]

40. Parambhath, V.B.; Nagar, R.; Ramaprabhu, S. Effect of Nitrogen Doping on Hydrogen Storage Capacity of Palladium Decorated Graphene. *Langmuir* **2012**, *28*, 7826–7833. [CrossRef]

41. Rusinque, B.; Escobedo, S.; de Lasa, H. Photoreduction of a Pd-Doped Meso-porous TiO$_2$ Photocatalyst for Hydrogen Production under Visible Light. *Catalysts* **2020**, *10*, 74. [CrossRef]

42. Mintcheva, N.; Aljulaih, A.A.; Wunderlich, W.; Kulinich, S.A.; Iwamori, S. La-ser-Ablated ZnO Nanoparticles and Their Photocatalytic Activity toward Organic Pollutants. *Materials* **2018**, *11*, 1127. [CrossRef] [PubMed]
43. Claros, M.; Setka, M.; Jimenez, Y.P.; Vallejos, S. AACVD Synthesis and Characterization of Iron and Copper Oxides Modified ZnO Structured Films. *Nanomaterials* **2020**, *10*, 471. [CrossRef] [PubMed]
44. Diculescu, V.C.; Beregoi, M.; Evanghelidis, A.; Negrea, R.F.; Apostol, N.G.; Enculescu, I. Palladium/palladium oxide coated electrospun fibers for wearable sweat pH-sensors. *Sci. Rep.* **2019**, *9*, 8902. [CrossRef] [PubMed]
45. Wu, Y.; Jiang, P.; Jiang, M.; Wang, T.-W.; Guo, C.-F.; Xie, S.-S.; Wang, Z.-L. The shape evolution of gold seeds and gold@silver core-shell nanostructures. *Nanotechnology* **2009**, *20*, 305602. [CrossRef] [PubMed]
46. Mao, S.; Zhao, B.; Wang, Z.; Gong, Y.; Guofeng, L.; Ma, X.; Yu, L.; Wang, Y. Tuning the Catalytic Performance for the Semi-hydrogenation of Alkynols by Selectively Poisoning the Active Sites of Pd Catalysts. *Green Chem.* **2019**, *21*, 4143–4151. [CrossRef]
47. Chen, X.; Shi, C.; Wang, X.B.; Li, W.-Y.; Liang, C. Intermetallic PdZn nanoparticles catalyze the continuous-flow hydrogenation of alkynols to cis-enols. *Commun. Chem.* **2021**, *4*, 175. [CrossRef]
48. Berguerand, C.; Yuranov, I.; Cárdenas-Lizana, F.; Yuranova, T.; Kiwi-Minsker, L. Size-Controlled Pd Nanoparticles in 2-Butyne-1,4-diol Hydrogenation: Support Effect and Kinetics Study. *J. Phys. Chem. C* **2014**, *118*, 12250–12259. [CrossRef]